

Supporting Information

Seeded on-Surface Supramolecular Growth for Large Area Conductive Donor-Acceptor Assembly

Goudappagouda,^a Sundaresan Chithiravel,^b Kothandam Krishnamoorthy,^b Suresh W. Gosavi,^c Sukumaran Santhosh Babu*^a

^a Organic Chemistry Division, CSIR-National Chemical Laboratory (CSIR-NCL), Pune-411008, India

^b Polymer Science and Engineering Division, CSIR-National Chemical Laboratory (CSIR-NCL), Pune-411 008, India

^c Department of Physics, Savitribai Phule Pune University, Pune-411 007, India

1. General	page S2
2. Experimental Procedure	page S2
3. Photographs, OM, FE-SEM and HR-TEM images of CHCl₃ assemblies	page S4
4. Photographs, OM, FE-SEM, HR-TEM and AFM images of THF assemblies	page S7
5. XRD and Raman spectra of TTF and TCNQ powders	page S14
6. UV-Vis-NIR spectra and STEM mapping images	page S15
7. OM and FE-SEM images of CHCl₃-THF assemblies	page S16
8. Conductivity	page S19
9. SAXS and References	page S22

1. General

Unless otherwise stated, solvents were purchased from commercial suppliers and used without further purification. Tetrathiafulvalene and tetracyano-*p*-quinodimethane was purchased from TCI and Sigma Aldrich, respectively. Raman spectroscopy studies were carried out using LabRAM HR with Ar laser (1500 nm) in the back scattering geometry. The detector was a Synapse CCD detector with thermoelectric cooling to $-70\text{ }^{\circ}\text{C}$. A 50 X (long distance) objective was used to focus the laser beam and to collect the Raman signal. The laser power on the sample was $\sim 2\text{ mW}$ (D1 filter), to avoid the possible heating effect by the laser on material surface. The size of the laser spot was $\sim 1\text{ }\mu\text{m}$. Zeta instruments optical microscope having 5x, 20x, 100x objective was used to image assembly samples. UV-Vis-NIR absorption was recorded on PerkinElmer Lambda-950 UV-Vis spectrometer. X-ray powder diffraction was acquired using a PANalytical X'PERT pro model the scan rate is $3\text{ }^{\circ}/\text{min}$ in the 2θ range of 5 to 50 degrees. AFM images were obtained using park systems XE 70 in non-contact mode. FE-SEM measurements were performed using a NOVA NANO SEM 450 (FEI) instrument operated at 10 to 15 kV. HR-TEM images were recorded on High Resolution Transmission Electron Microscope (HRTEM) 200kV with Field Emission, TECNAI G2 20 TWIN, FEI under 200 KV. Conductivity values were measured by Agilent 4156 C semiconductor probe analyzer in N_2 environment. The micropatterend substrates for conductivity measurements were purchased from Fraunhofer Institute for Photonic Microsystems IPMS, Dresden, Germany. The video image of the on-surface extended assembly formation was recorded on Nikon LV150NL Trinocular upright optical microscope. Small angle X-ray scattering experiments measurements were performed on a Bruker Nanostar equipped with a rotating anode generator (18 kW) operated at a voltage of 45 kV and current of 18 mA. The X-rays are collimated through a three-pinhole system, and data is acquired using a 2D gas filled HiStar detector.

2. Experimental Procedure

2a. TTF-TCNQ dendritic-sheaf assembly.

CHCl_3/THF

TTF-TCNQ dendritic-sheaf was prepared as 0.5 ml of equimolar CHCl_3/THF solutions of TTF and TCNQ were simultaneously mixed at ambient condition. The resulting solution was allowed to stand over 5 min without disturbance. A drop (10 μL) of a TTF-TCNQ solution was placed on silicon/glass substrates and dried over 2 min. The dendritic-sheaf structures formed were investigated by OM, FE-SEM and HR-TEM. In CHCl_3 , sheaf-like structures were formed at 2-10 mM and samples obtained at 3 mM were mainly considered for all the experiments. Whereas in THF, dendritic-sheaf was formed only at higher concentrations, 7-10 mM.

2b. TTF-TCNQ Assembly on surface.

THF

0.5 ml of equimolar THF solutions of TTF and TCNQ were simultaneously mixed at ambient condition. The resulting solution was allowed to stand over 5 min without disturbance. A drop (5 μL) of a TTF-TCNQ mixed THF solution was placed on silicon/glass substrates and dried over 2 min. The extended fiber formation starting from the living termini of sheaf formed in solution was observed on solid substrate after solvent evaporation.

CHCl_3+THF

A Drop (2/5 μL) of TTF-TCNQ dendritic-sheaf formed in CHCl_3 was placed on silicon substrate and dried over 2 min. And onto the dried sample, THF solution (2/5 μL) of TTF and TCNQ (1:1) was added carefully and the solvent was allowed to evaporate in 2 min. The extended fiber formation starting from the living termini of CHCl_3 sheaf was observed on solid substrate after solvent evaporation.

2c. Samples for OM, FE-SEM and AFM

The OM, FE-SEM and AFM samples were prepared by drop casting (10 μL) of the assembly solution on silicon/glass substrates and dried over 2 min. After complete evaporation of the solvent, samples were directly used for OM and AFM analyses. The samples were coated with Pt/Cr in an ion coater for 5 min before FE-SEM analysis.

2d. Samples for HR-TEM

The samples for HR-TEM were prepared by drop casting the assembly solutions in CHCl_3 and THF on carbon coated Cu grid and allowed to dry for 2 min.

2e. Samples for XRD, Raman and UV-Vis-NIR Spectra

Equimolar CHCl_3 /THF solutions of TTF and TCNQ were simultaneously mixed at ambient condition and the samples were allowed to settle for 20 min. The supernatant solution was removed and the remaining solvent was evaporated under ambient condition and finally dried under vacuum.

2f. Electrical Characterization

I/V measurement was performed by drop casting the assembly solution on n-doped Si/SiO₂ (230 \pm 10 nm, 14.9 nF) containing ITO adhesion layer (10 nm) on that Au pads having thickness of 30 nm are deposited. The electrodes were purchased from Fraunhofer Institute for Photonic Microsystems IPMS, Dresden, Germany. The CHCl_3 /THF solutions (10 mM, 100 μL) were drop-casted onto the Au pads of Si/SiO₂ substrate at ambient condition. The electrodes have been moved to glove box after sample deposition. The measurements were carried out using Au electrodes with 10/20 μm channel length and 0.5 mm channel width using Agilent 4156 C semiconductor probe analyser in Ar environment.

The conductivity values were calculated using the following equations.

Resistance (R) = V/I Ω ; where V = voltage and I = current

Resistivity (ρ) = R · A/l $\Omega\cdot\text{cm}$; where A = Area of the channel and l = length of the channel

Conductivity (σ) = 1/ ρ Scm^{-1}

2g. Samples for supporting video

A video image was recorded by drop casting THF solution (3 mM, 10 μL) of TTF and TCNQ (1:1) on glass substrate. After placing the droplet on glass substrate, the solvent front moved from the edges to the centre of the substrate within 10 sec and the complete solvent evaporation occurred within 1.5 min.

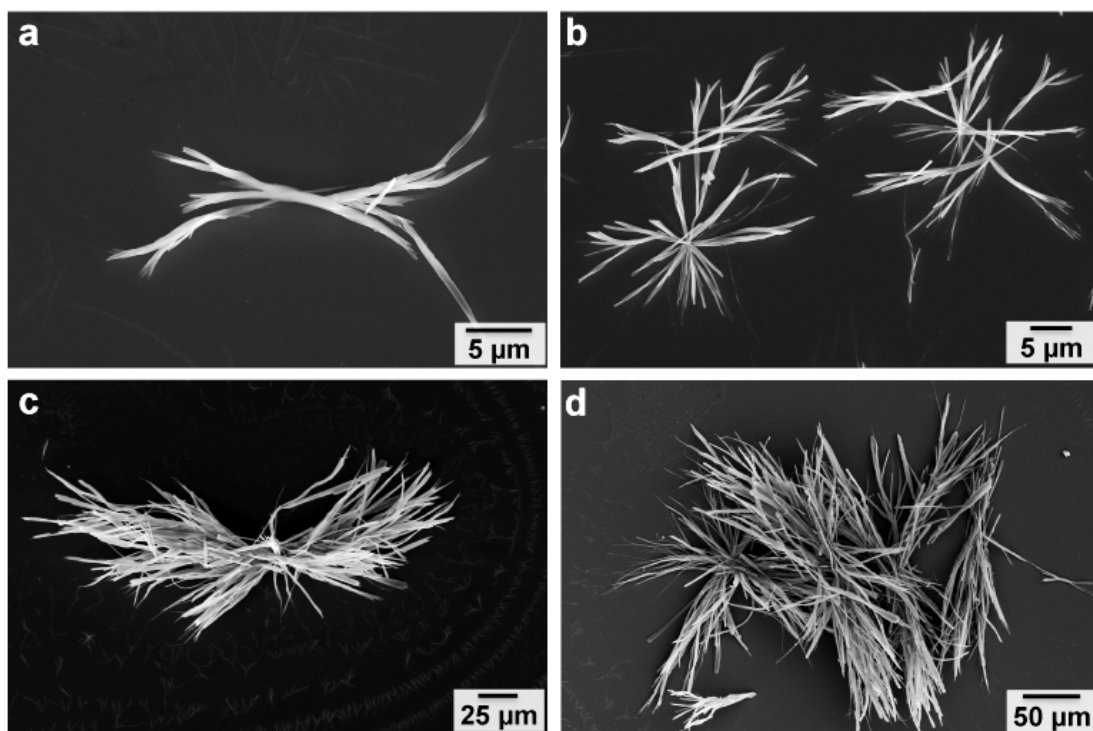


Fig. S1. FE-SEM images of the TTF-TCNQ assembly obtained by simultaneous addition of CHCl_3 solutions (0.5 mL each) of TTF and TCNQ and drop casted (10 μL) on silicon substrate. a), b) 1 mM, c), d) 3 mM.

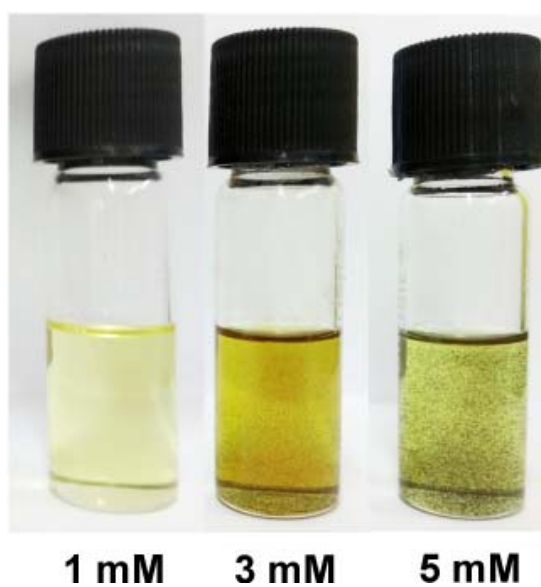


Fig. S2. Photographs of the concentration dependent visible changes upon simultaneous addition of CHCl_3 solutions (0.5 mL each) of TTF and TCNQ.

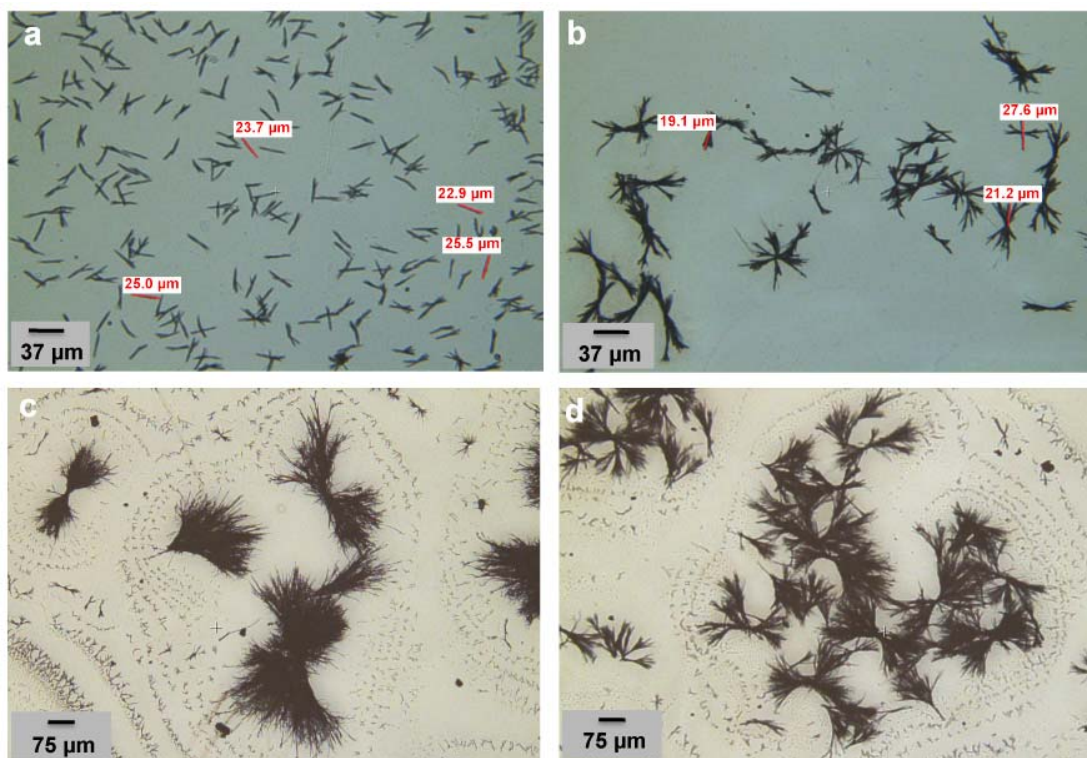


Fig. S3. OM images of the TTF-TCNQ assembly obtained by simultaneous addition of CHCl_3 solutions (0.5 mL each) of TTF and TCNQ and drop casted (10 μL) on silicon substrate. a) 0.5 mM, b) 2 mM, c) 3 mM and d) 5 mM.

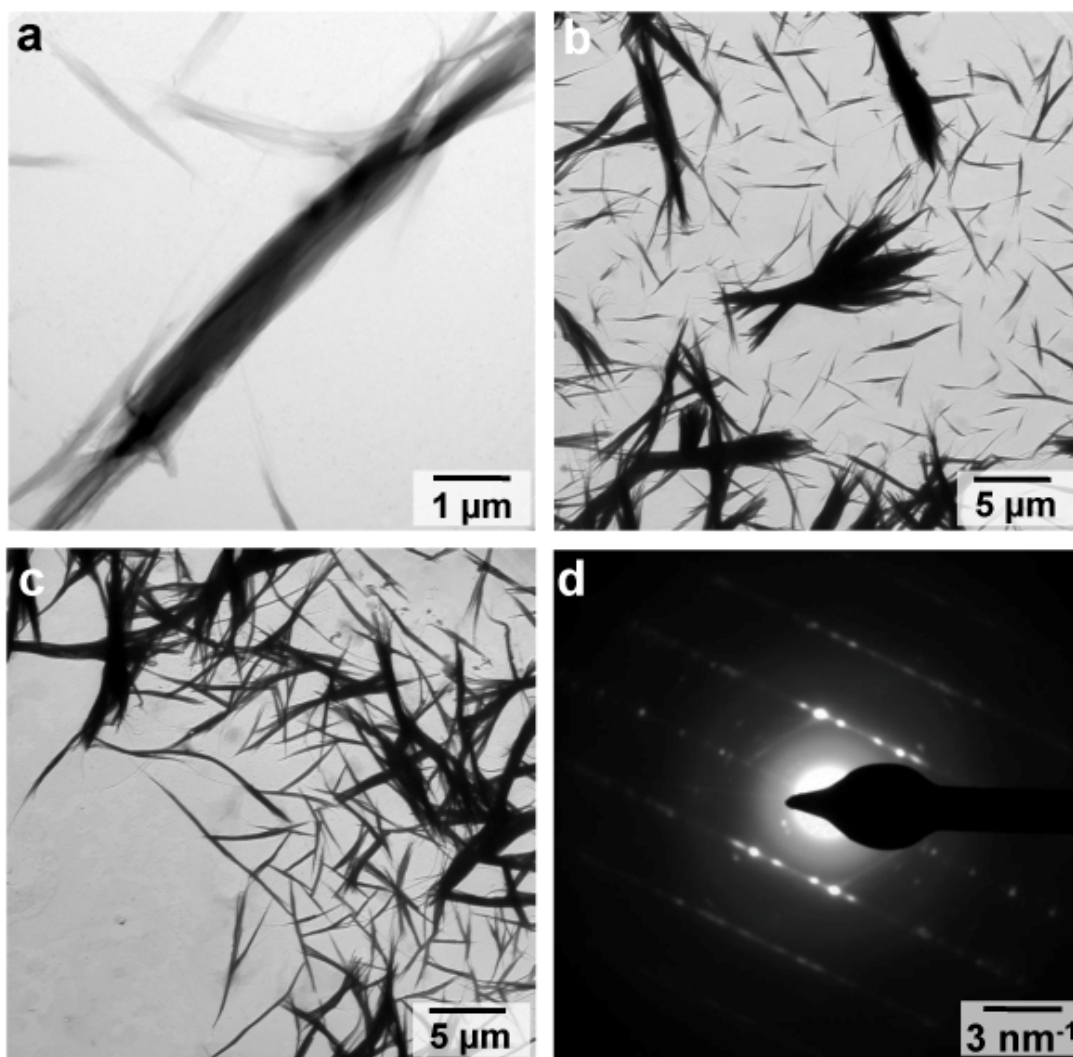


Fig. S4. a)-c) HR-TEM images of the TTF-TCNQ assembly obtained by simultaneous addition of CHCl_3 solutions (5 mM, 0.5 mL each) of TTF and TCNQ and drop casting the supernatant solution on a carbon coated copper grid. d) SAED pattern of an individual sheaf leaf indicating the higher order of crystallinity in the sample.

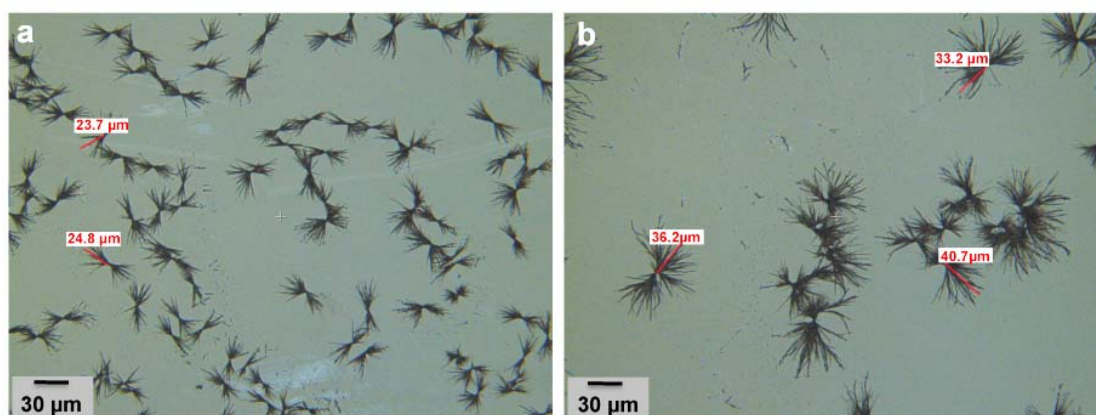


Fig. S5. OM images of the TTF-TCNQ assembly in CHCl_3 drop casted (10 μL) on glass substrate. a) Dendritic-sheaf formed by simultaneous addition of CHCl_3 solutions (1.5 mM, 0.5 mL each) of TTF and TCNQ and b) after simultaneous addition of extra CHCl_3 solution (1.5 mM, 100 μL each) of TTF and TCNQ and waiting for 2 hours.

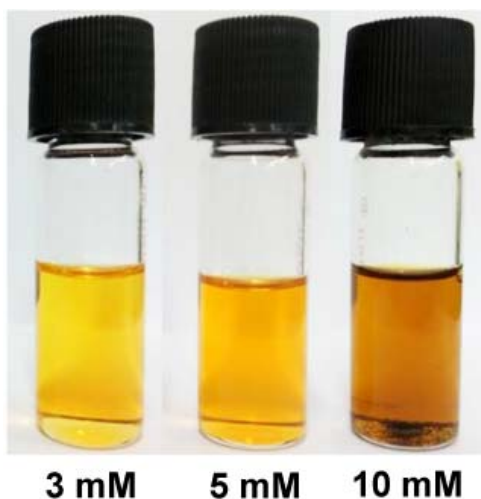


Fig. S6. Photographs of the concentration dependent visible changes upon simultaneous addition of THF solutions (0.5 mL each) of TTF and TCNQ.

The color change for TTF-TCNQ in THF was not so predominant for 1-5 mM, on the other hand at 10 mM a dark brown color appeared with partial precipitation.

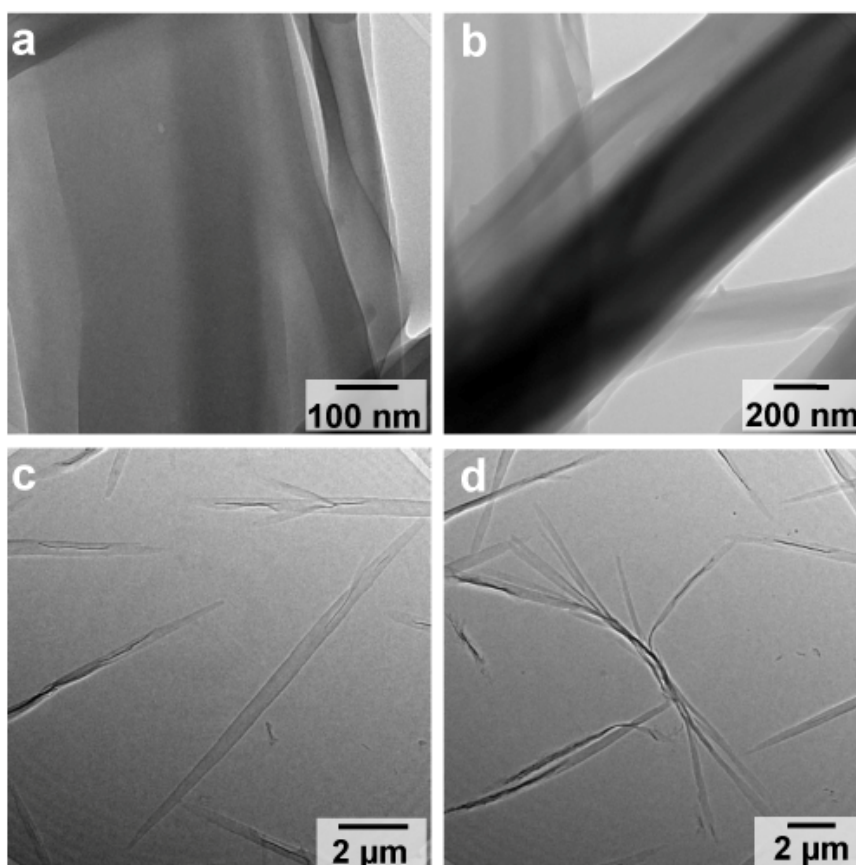


Fig. S7. a)-d) HR-TEM images of the TTF-TCNQ assembly obtained by simultaneous addition of THF solutions (2 mM, 0.5 mL each) of TTF and TCNQ and drop casting the supernatant solution on a carbon coated copper grid.

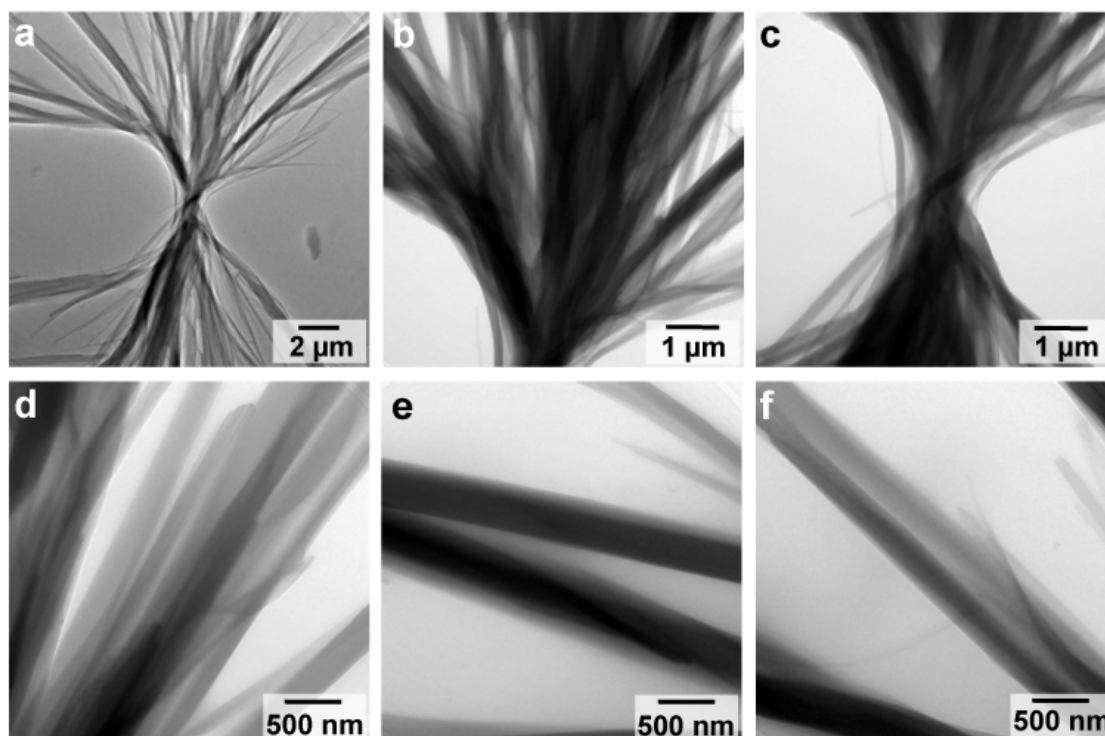


Fig. S8. a)-f) HR-TEM images of the TTF-TCNQ assembly obtained by simultaneous addition of THF solutions (2 mM, 0.5 mL each) of TTF and TCNQ and drop casting the supernatant solution on a carbon coated copper grid.

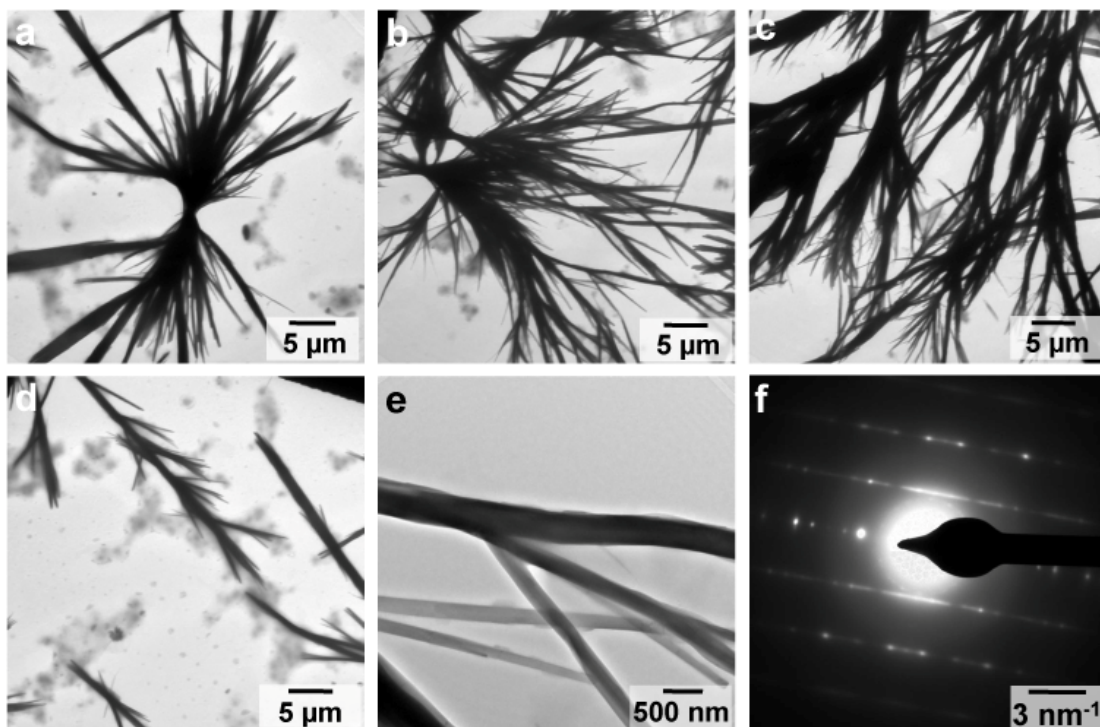


Fig. S9. a)-e) HR-TEM images of the TTF-TCNQ assembly obtained by simultaneous addition of THF solutions (5 mM, 0.5 mL each) of TTF and TCNQ and drop casting the supernatant solution on a carbon coated copper grid. f) SAED pattern of an individual fiber grown from the sheaf leaf.

The extended on-surface assembly formation from THF solution is found to be concentration and substrate dependent. An optimum concentration of 3-10 mM was found to be ideal for the assembly formation. Substrate such as silicon and glass were supportive whereas mica doesn't initiate the assembly formation upon evaporation. Surprisingly, HR-TEM image (5 mM) shows that fiber growth was observed on carbon coated Cu grid also, but growth was limited only to a few ten micrometers.

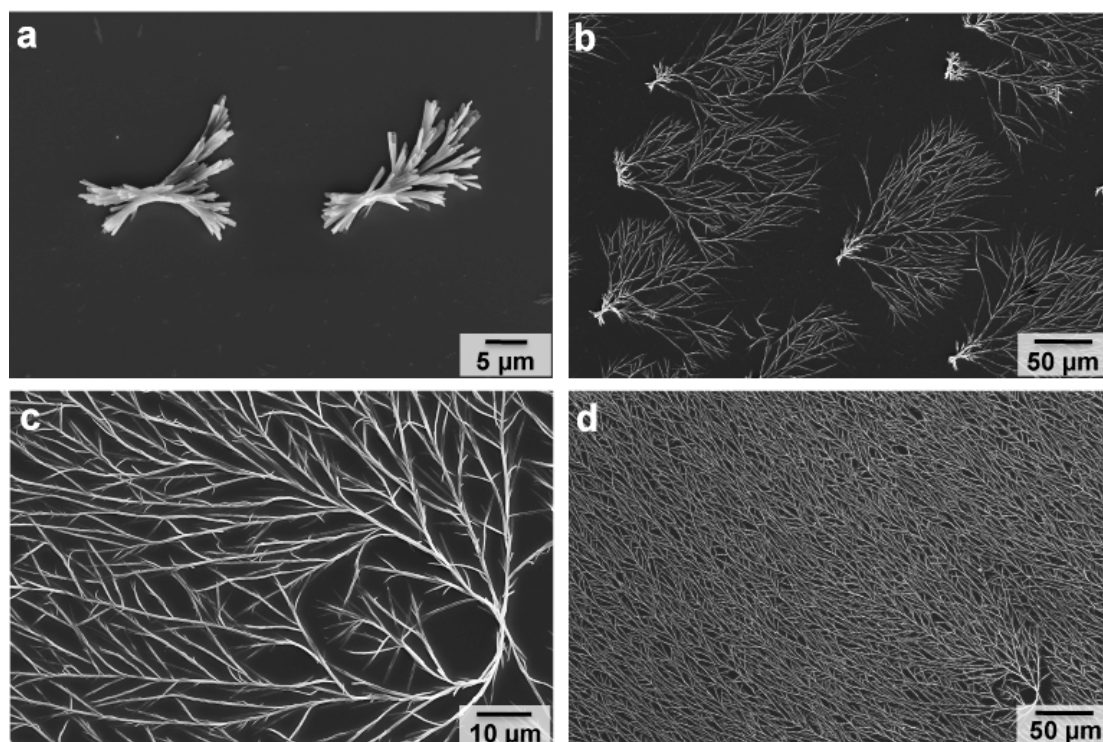


Fig. S10. FE-SEM images of the TTF-TCNQ assembly obtained by simultaneous addition of THF solutions (0.5 mL each) of TTF and TCNQ and drop casting (10 μ L) on silicon substrate. a), b) 3 mM and c), d) 5 mM.

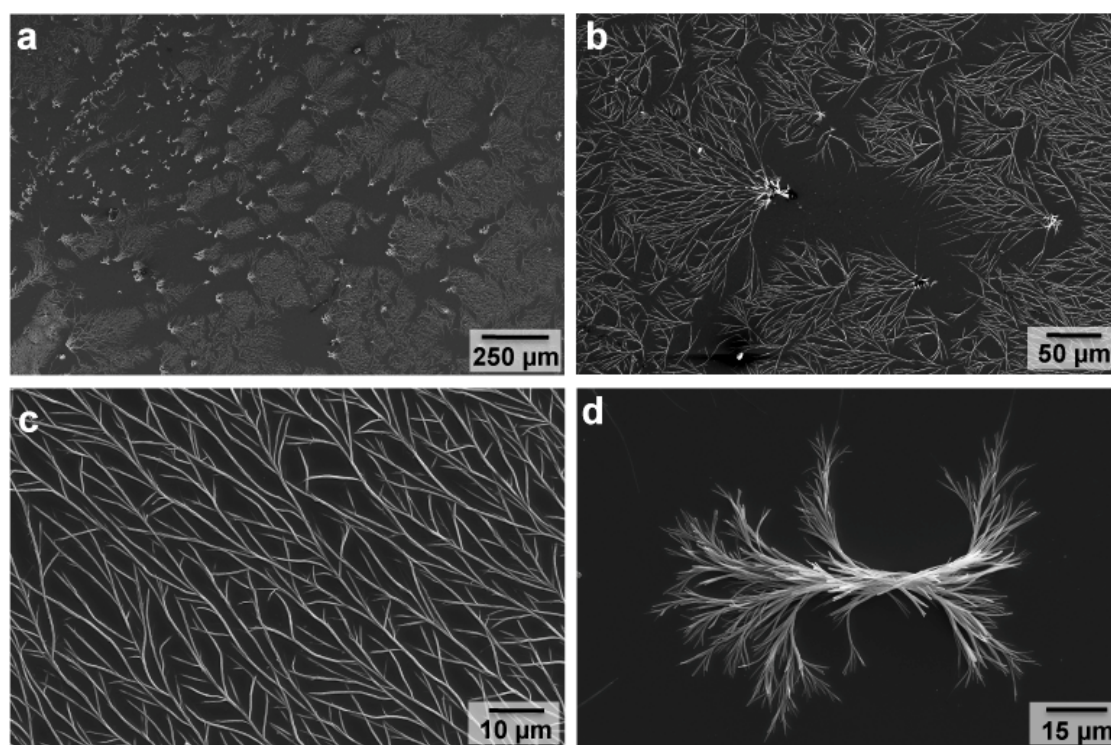


Fig. S11. FE-SEM images of the TTF-TCNQ assembly obtained by simultaneous addition of THF solutions (0.5 mL each) of TTF and TCNQ and drop casting (10 μ L) on silicon substrate. a), b) 3 mM and c), d) 5 mM.

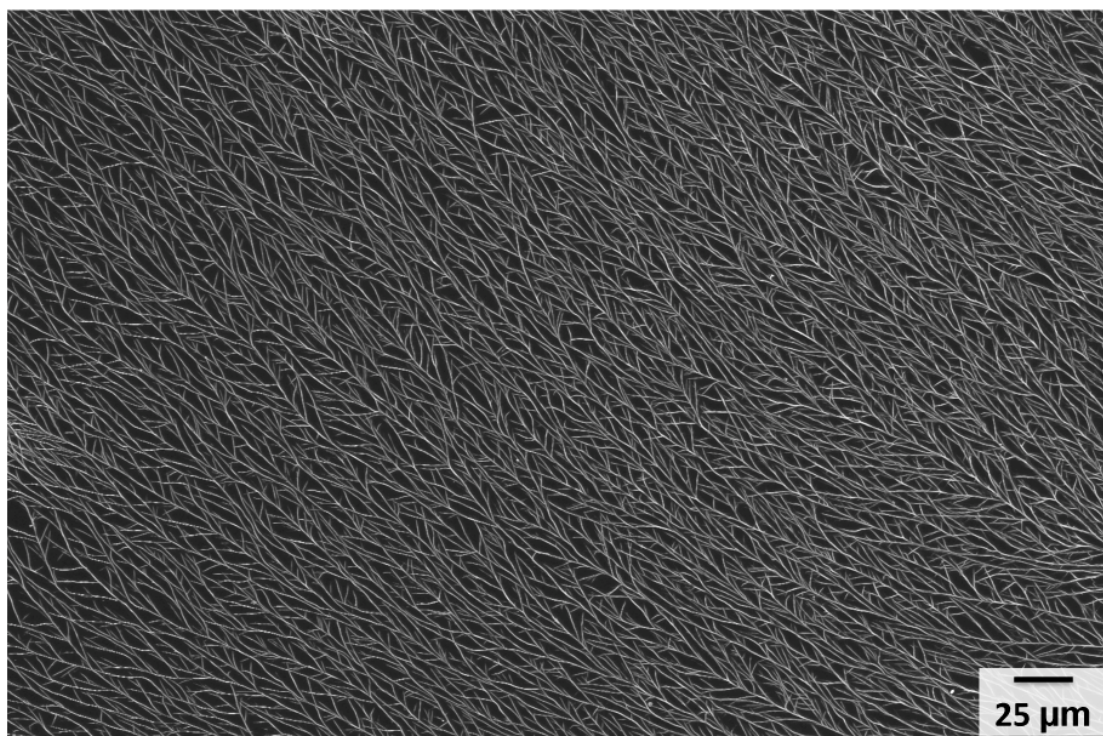


Fig. S12. FE-SEM images of the TTF-TCNQ assembly obtained by simultaneous addition of THF solutions (5 mM, 0.5 mL each) of TTF and TCNQ and drop casting (10 μL) on silicon substrate.

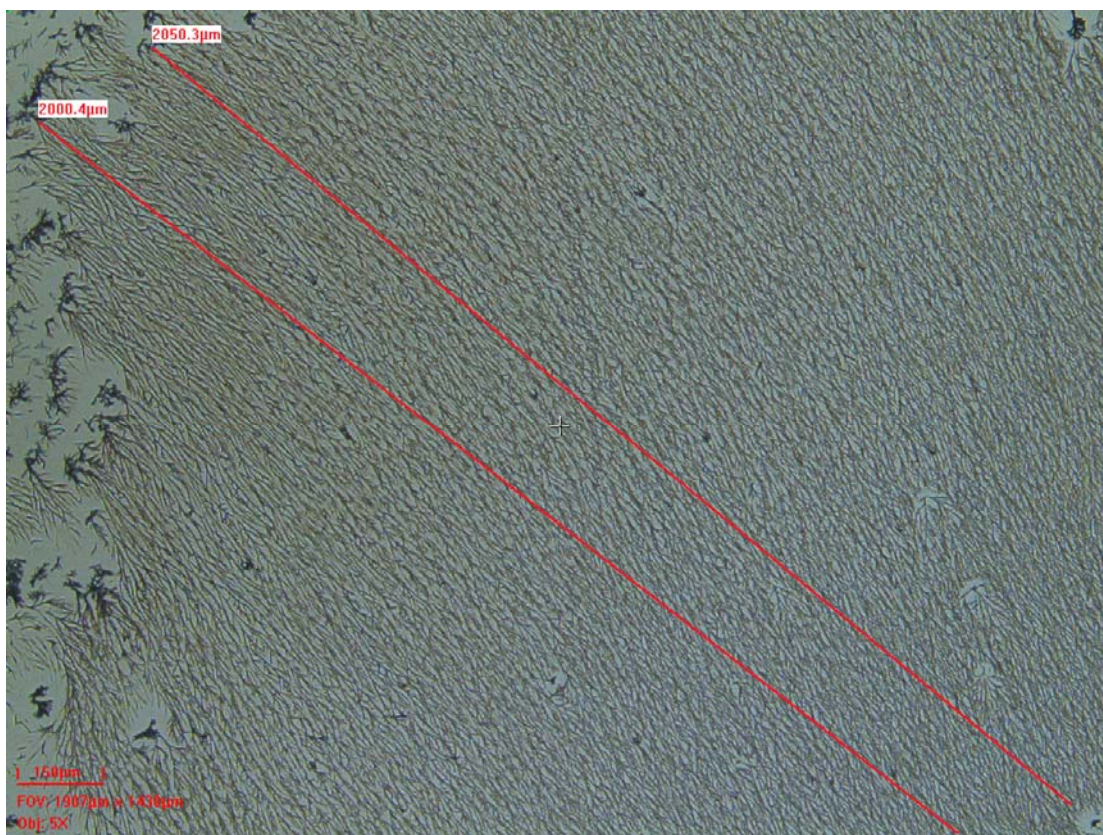


Fig. S13. OM images of the TTF-TCNQ assembly obtained by simultaneous addition of THF solutions (5 mM, 0.5 mL each) of TTF and TCNQ and drop casting (10 μL) on silicon substrate.

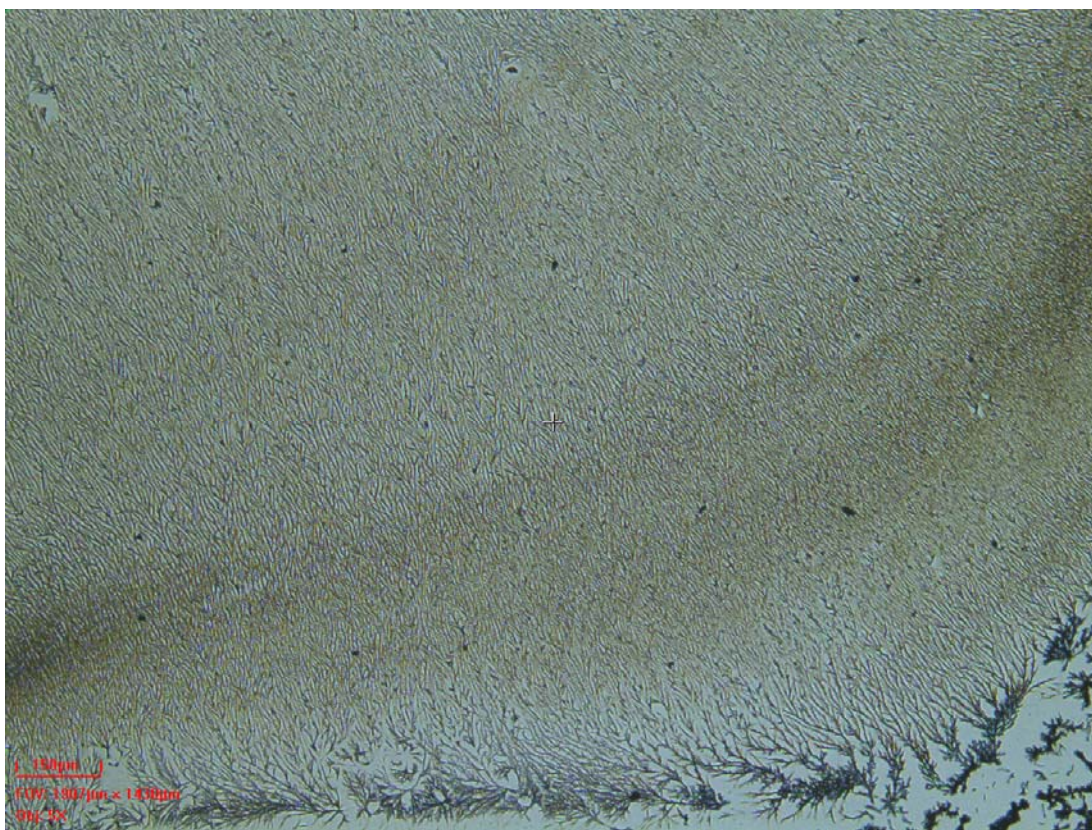


Fig. S14. OM images of the TTF-TCNQ assembly obtained by simultaneous addition of THF solutions (5 mM, 0.5 mL each) of TTF and TCNQ and drop casting (10 μ L) on silicon substrate.

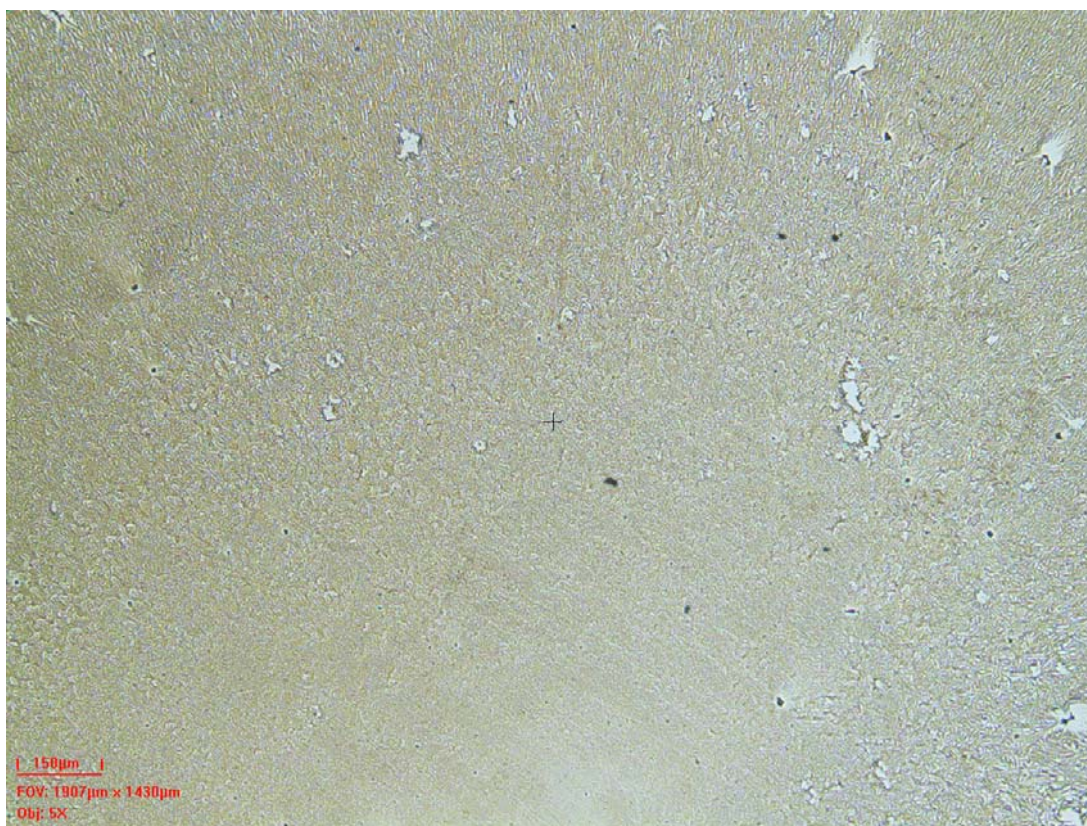


Fig. S15. OM images of the TTF-TCNQ assembly obtained by simultaneous addition of THF solutions (5 mM, 0.5 mL each) of TTF and TCNQ and drop casting (10 μ L) on silicon substrate.

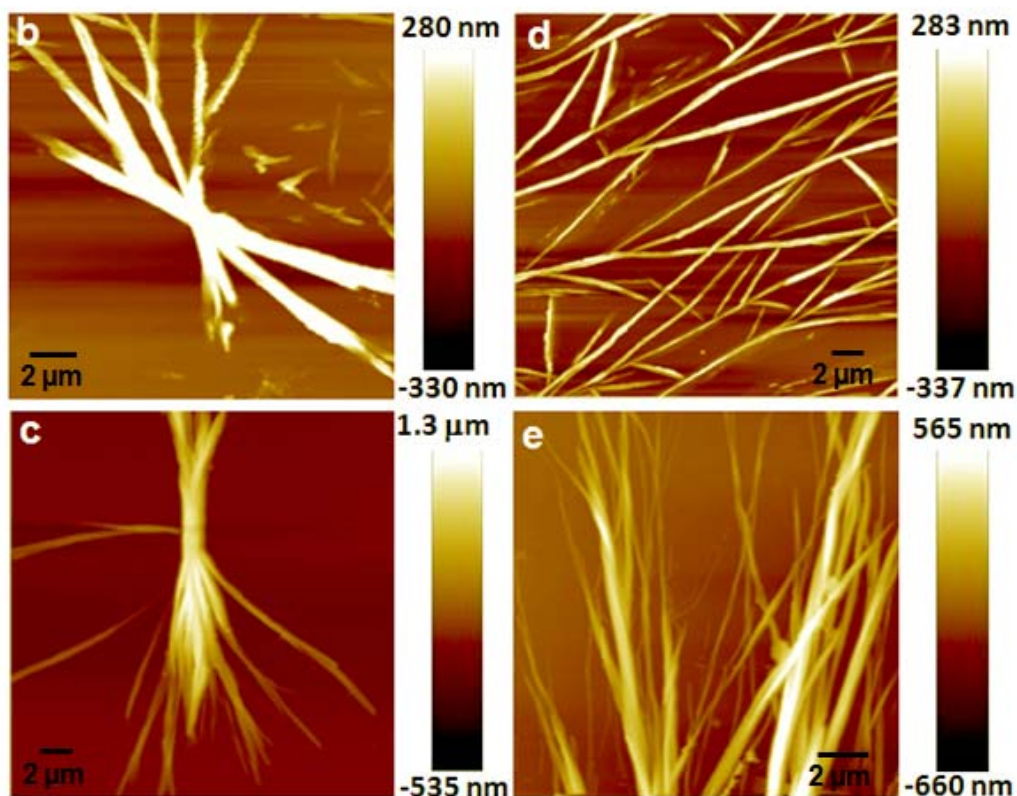
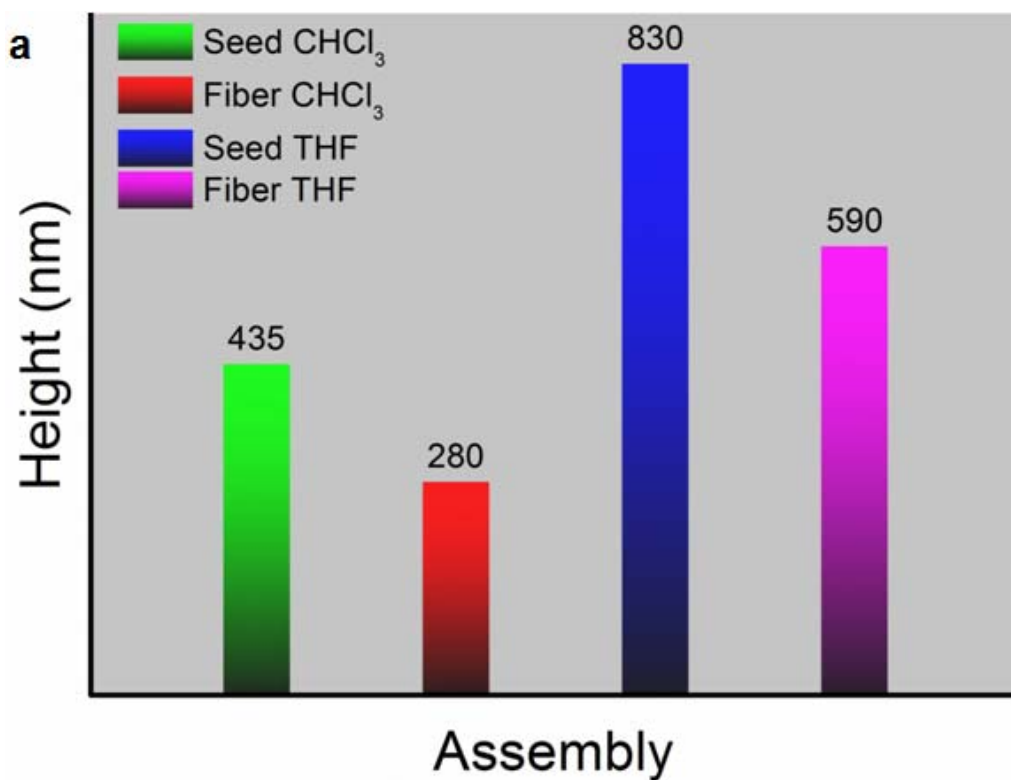


Fig. S16. a) Histogram of the height profiles obtained from AFM images of b), c) seeds and d), f) fibrous assembly obtained by simultaneous addition of THF solutions 5 mM (top) and 10 mM (bottom) of TTF and TCNQ and drop casting (10 μL) on silicon substrate.

The height profile comparison (based on 10 different measurements) of the seeds and fibrous assembly well correlates with concentration of TTF-TCNQ solution. As the seed size is increased, the height/size of the corresponding fibrous assembly also exhibited an increment. AFM analysis of sample at very high concentration (10 mM) was not possible due to the larger size of the assembly and hence the imaging and histogram analysis has been done on smaller sheaf and fibers formed.

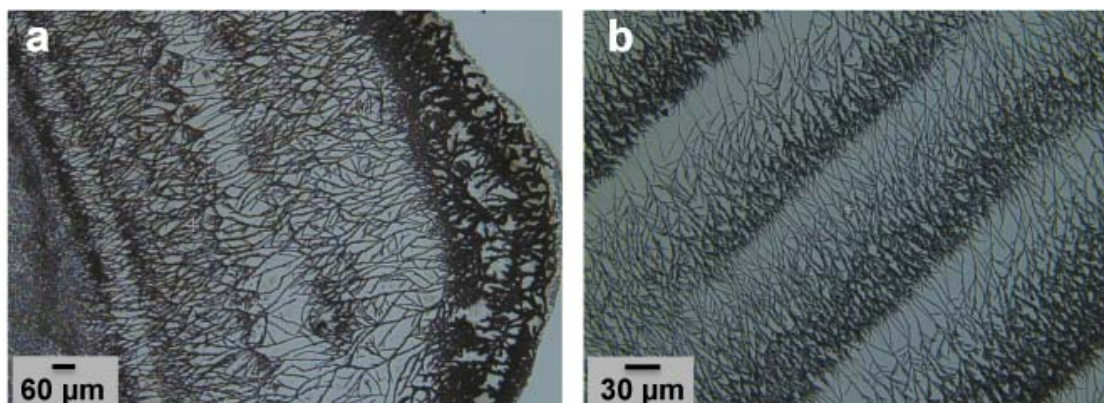


Fig. S17. a), b) OM images of the TTF-TCNQ assembly obtained by simultaneous addition of THF solutions (5 mM, 0.5 mL each) of TTF and TCNQ and drop casting (10 μ L) on silicon substrate.

At higher concentrations, seeded growth leads to the formation of discontinuous fibrous structures having a dendritic feature at the edge parts of the substrate (for a minor extent) due to faster solvent evaporation at the edges.^{S1} This is observed only at the edge parts where islands of excess solvent located. One point to be noticed is that in this case also the solution formed seeds initiate the growth on surface.

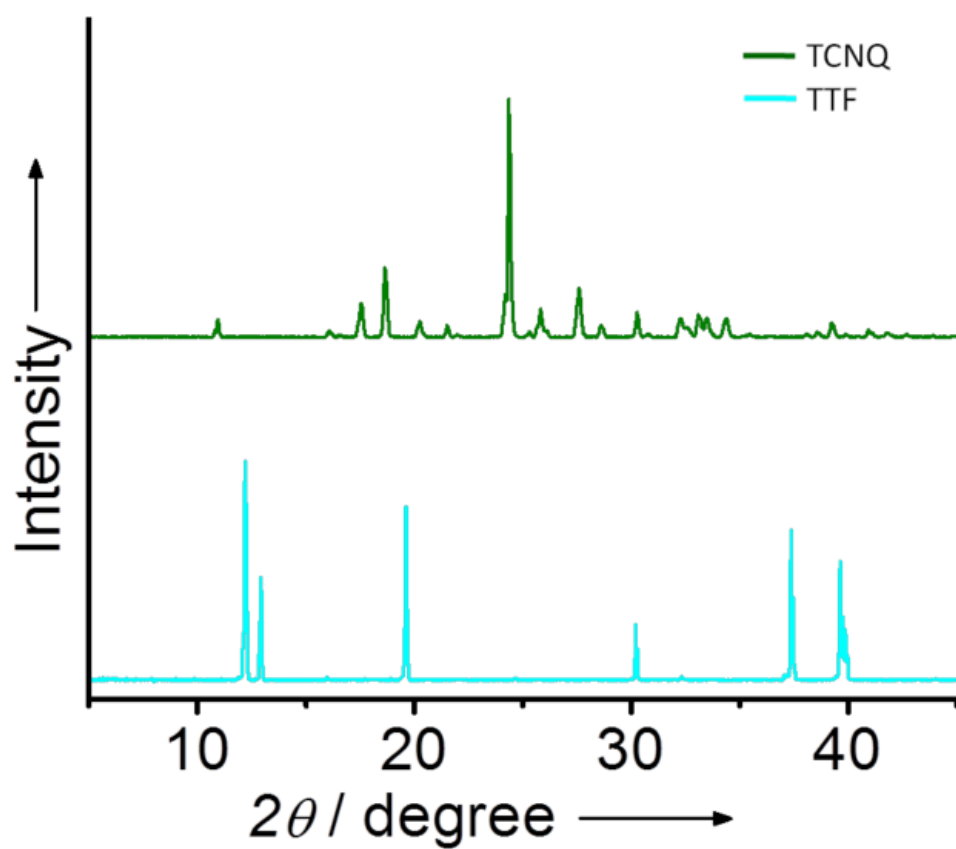


Fig. S18. XRD spectra of TTF and TCNQ powders.

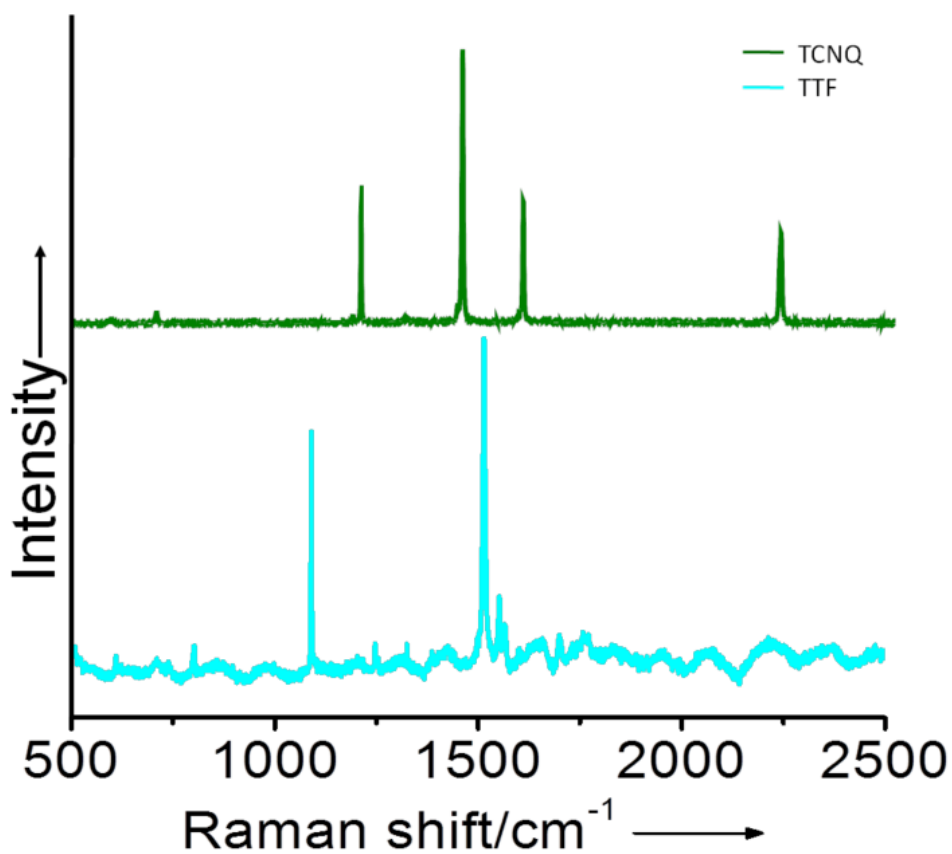


Fig. S19. Raman spectra of TTF and TCNQ powders.

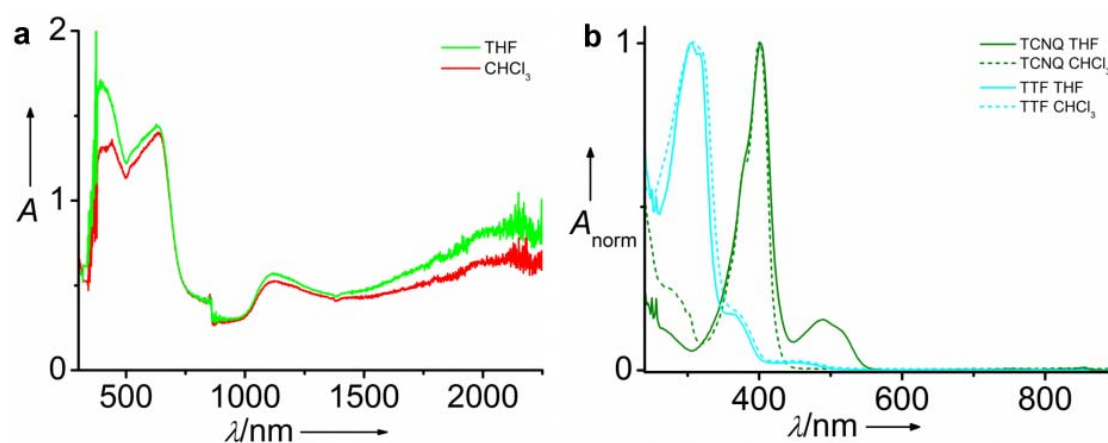


Fig. S20. a) Solid state UV-Vis-NIR spectra of TTF-TCNQ assemblies from CHCl_3 and THF. b) Normalized UV-Vis-NIR spectra of TTF and TCNQ in CHCl_3 and THF.

The presence of a new characteristic CT band between 1000 and 2250 nm in the spectrum is a clear evidence for the CT interaction between TTF and TCNQ in the assemblies both in THF and CHCl_3 .

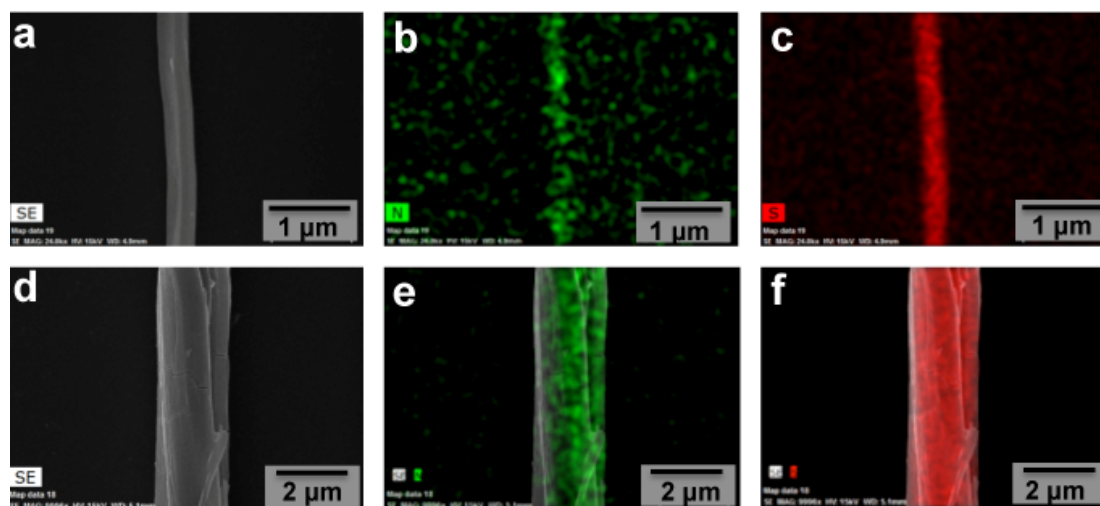


Fig. S21. a), d) SEM image and corresponding STEM mapping images for b), e) nitrogen and c), f) sulfur of the seeded on-surface grown TTF-TCNQ fibers from THF (5 mM) (top) and by sequential deposition of THF solution (5 μ L, 3 mM) of TTF and TCNQ on CHCl_3 sheaf (5 μ L, 10 mM) (bottom), respectively, on silicon substrate.

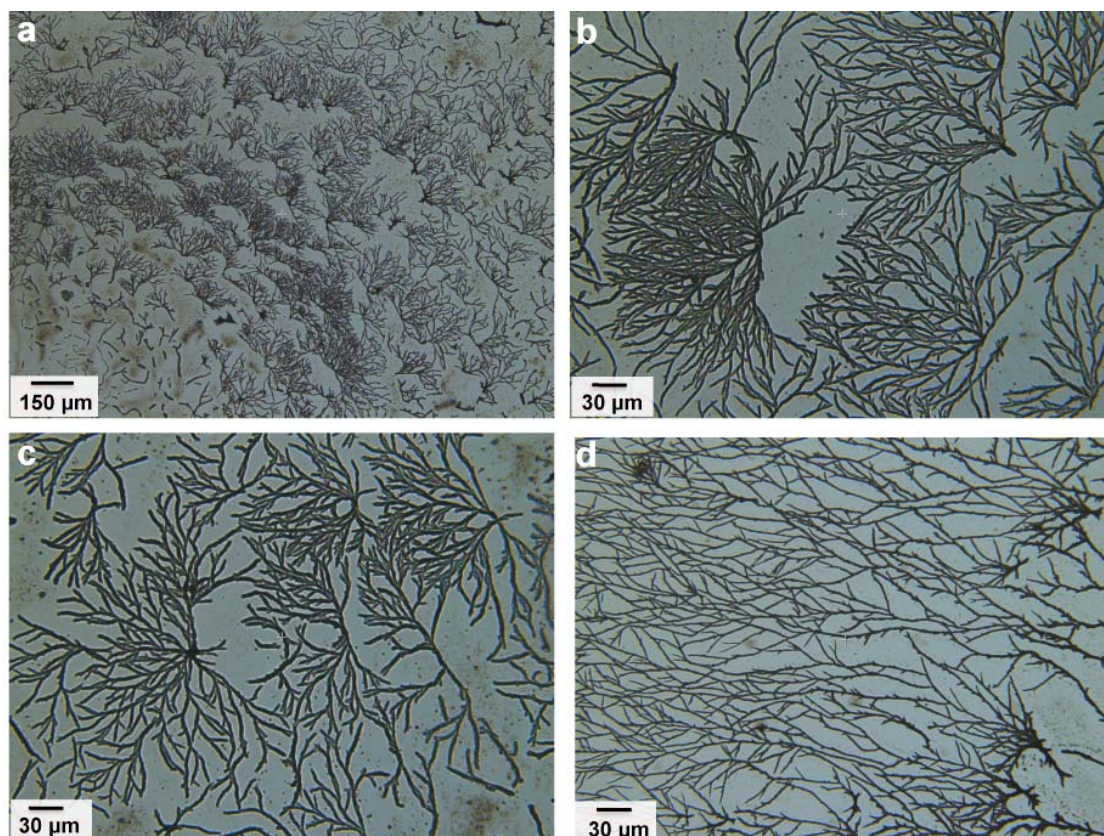


Fig. S22. a-d) OM images of seeded supramolecular polymers of TTF-TCNQ obtained by sequential deposition of THF solution (2 μ L, 1 mM) of TTF and TCNQ on already deposited CHCl_3 sheaves (2 μ L, 5 mM) on silicon substrate.

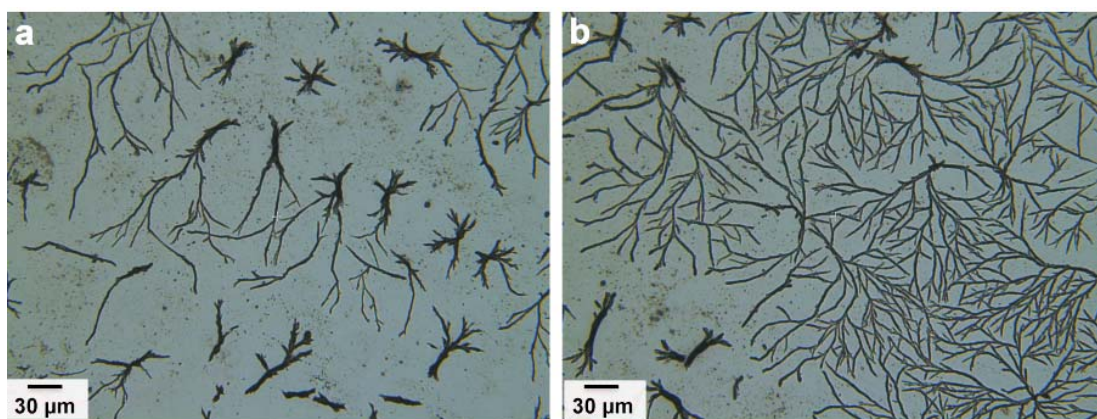


Fig. S23. a), b) OM images of seeded supramolecular polymers of TTF-TCNQ obtained by sequential deposition of THF solution (2 μL , 1 mM) of TTF and TCNQ on already deposited CHCl_3 sheaves (2 μL , 3 mM) on silicon substrate.

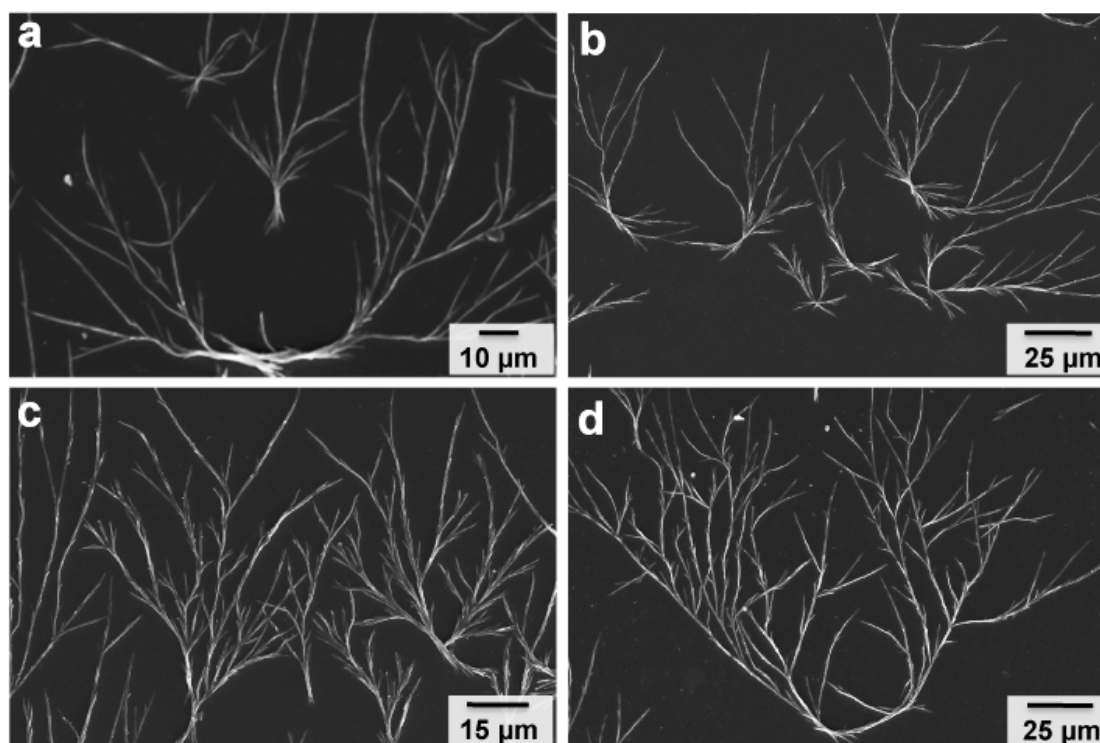


Fig. S24. a)-d) FE-SEM images of seeded supramolecular polymers of TTF-TCNQ obtained by sequential deposition of THF solution (2 μL , 3 mM) of TTF and TCNQ on already deposited CHCl_3 sheaves (2 μL , 10 mM) on silicon substrate.

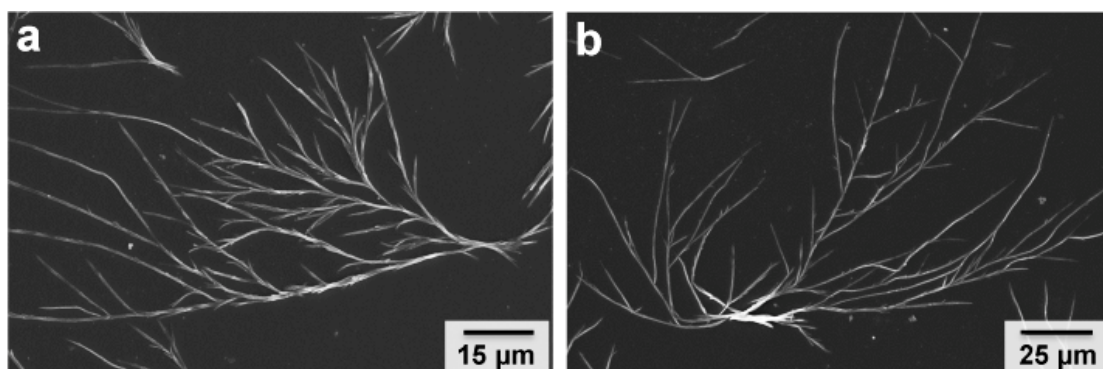


Fig. S25. a), b) FE-SEM images of seeded supramolecular polymers of TTF-TCNQ obtained by sequential deposition of THF solution (2 μL , 3 mM) of TTF and TCNQ on already deposited CHCl_3 sheaves (2 μL , 10 mM) on silicon substrate.

Table S1. Comparison of the conductivity of reported TTF-TCNQ assemblies.

Entry	Conductivity	Assembly type	Reference
1	$10^6 \text{ ohm}^{-1}\text{cm}^{-1}$	Crystals	<i>Solid State Comm.</i> 1973 , 12, 1125.
2	$1.47 \times 10^4 \text{ ohm}^{-1}\text{cm}^{-1}$ at 66 K	Crystals	<i>J. Am. Chem. Soc.</i> 1973 , 95, 948.
3	600, 1, and 10^{-3} Scm^{-1} along the b, c, and a directions, respectively	Crystals	<i>Phys. Rev. B</i> 1974 , 10, 1298.
4	$500 \text{ ohm}^{-1}\text{cm}^{-1}$ at 58 K	Crystals	<i>J. Phys. Soc. Jpn.</i> 1976 , 41, 351.
5	5:0 Scm^{-1} (#1a), 9:1 Scm^{-1} (#1b) and 2:2 Scm^{-1} (#3)	Polycrystalline thin films by thermal sublimation films obtained under different experimental conditions: (#1) $T_s = 300 \text{ K}$ and $T_a = 350 \text{ K}$, (#2) $T_s = 310 \text{ K}$, and $T_a = 360 \text{ K}$ and (#3) $T_s = 325 \text{ K}$ and $T_a = 350 \text{ K}$. T_s = substrate temperature, T_a = annealing temperature	<i>J. Solid State Chem.</i> 2002 , 168, 384.
6	$3.8 \times 10^{-4} \text{ Scm}^{-1}$ at bias voltages below 1 V, and $1.05 \times 10^{-2} \text{ Scm}^{-1}$ at bias voltages above 4 V	Helical nanowires	15c
7	$0.01\text{-}0.1 \text{ Scm}^{-1}$	Nanoparticle powder	<i>Langmuir</i> 2013 , 29, 8983.
8	$1.5 \pm 0.9 \times 10^{-5} \text{ Scm}^{-1}$ $2.9 \pm 0.9 \times 10^{-5} \text{ Scm}^{-1}$	Nanofibers	10c
9	$7.0 \pm 3.0 \times 10^{-4} \text{ Scm}^{-1}$	Helical nanofiber	10b
10	1 Scm^{-1}	Bundle of nanowires	<i>Acad. Sci. Paris, Ser. IIC</i> 2000, 3, 675.
11	0.11×10^{-2} and $0.09 \times 10^{-2} \text{ Scm}^{-1}$	Branched fibers	This study

Table S1 indicates that the present study has delivered TTF-TCNQ assemblies with comparatively better conductivity values. The highest values so far reported are exhibited by high quality single/poly crystalline assemblies prepared by thermal evaporation.

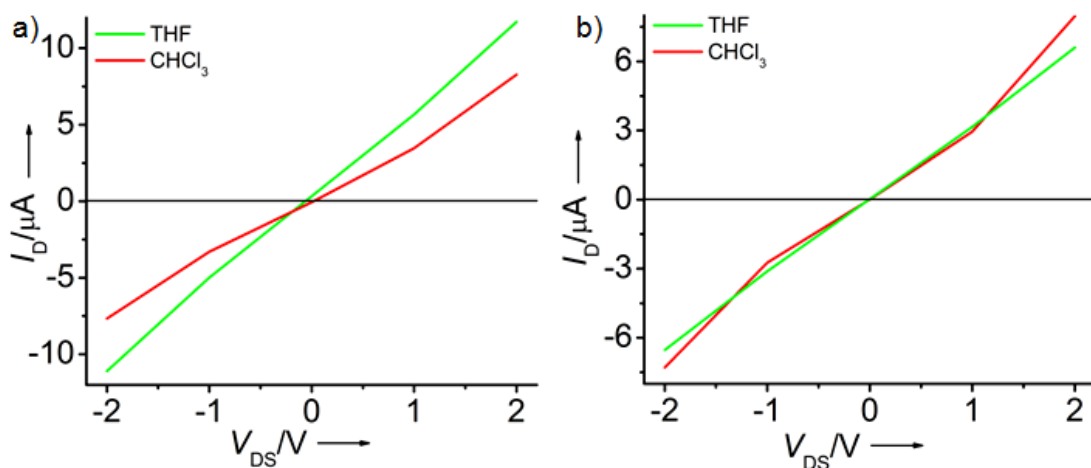


Fig. S26. I-V curves for TTF-TCNQ assemblies with maximum conductivity values obtained from THF and CHCl_3 (5 mM) deposited on Au electrodes with channel widths of a) 10 μm and b) 20 μm .

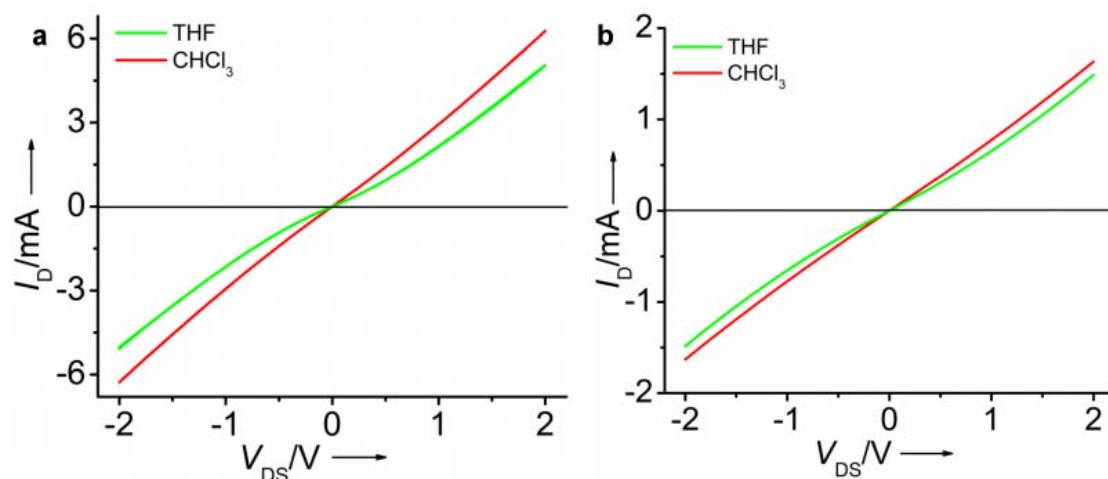


Fig. S27. I-V curves for TTF-TCNQ assemblies with average conductivity values obtained from THF and CHCl_3 (10 mM) deposited on Au electrodes with channel widths of a) 10 μm and b) 20 μm .

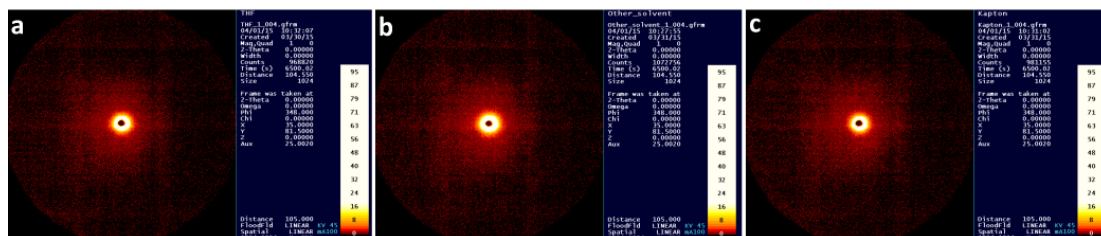
Table S2. Comparison of the average conductivity value of TTF-TCNQ assemblies in CHCl_3 and THF (5 and 10 mM) by depositing on Au electrodes with channel widths of 10 and 20 μM , values obtained from 10 different measurements.

Assembly	Concentration	Channel Widths	
		10 μM	20 μM
	5 mM		
CHCl_3		$0.35 \times 10^{-6} \text{ Scm}^{-1}$	$0.19 \times 10^{-6} \text{ Scm}^{-1}$
THF		$0.24 \times 10^{-6} \text{ Scm}^{-1}$	$0.1 \times 10^{-6} \text{ Scm}^{-1}$
	10 mM		
CHCl_3		$0.2 \times 10^{-2} \text{ Scm}^{-1}$	$0.1 \times 10^{-2} \text{ Scm}^{-1}$
THF		$0.13 \times 10^{-2} \text{ Scm}^{-1}$	$0.07 \times 10^{-2} \text{ Scm}^{-1}$

As shown in Table S2, the maximum conductivity values were obtained for assemblies formed at higher concentration of TTF-TCNQ (10 mM). One point to be noticed is the size/height variation of the fibrous assembly with concentration (Fig. S17) and as the concentration is increased, thicker and larger fibers are formed. This may help to cover the entire channel area, well bridging with the Au electrodes and resulting in higher conductivity.

Molecular orientation of fibers on surface

In order to understand the molecular orientation of the fibers formed on surface, small angle X-ray scattering (SAXS) experiment has been performed. The branched fibers obtained by drop casting THF solution (1 mL, 5 mM) on Kapton film failed to show any specific diffraction pattern. Due to the inhomogeneity and insufficient covering of the surface by the fibrous structure, scattering from the surface dominates over the signals from the sample.



SAXS profile of on-surface assembly from a) THF and b) CHCl₃ and c) substrate alone. The samples were prepared by multiple deposition of the assembly solution (1 mL, 5 mM) on Kapton film.

4. References

- S1. Mukherjee, B.; Mukherjee, M. *Langmuir* **2011**, *27*, 11246.